

# Thermophysical Properties of Binary Mixtures of Methyl Methacrylate + Di-Ethers (Ethyl, Isopropyl, and Butyl) at 298.15 and 308.15 K

J. George<sup>1</sup> and N. V. Sastry<sup>1,2</sup>

*Received January 27, 2003*

---

Experimental data for the densities, dynamic viscosities, sound speeds, and relative permittivities and for three binary systems of methyl methacrylate (MMA) + di-ethers (ethyl, isopropyl, and butyl) at 298.15 and 308.15 K and at atmospheric pressure are reported. The mixture viscosities are correlated by Grunberg–Nissan, McAllister, and Auslander equations over the complete composition range. The sound speeds for the mixtures are also calculated by using free length and collision factor theories, and Nomoto and Junjie equations. From the measured primary properties, deviation functions such as deviations in viscosities, sound speeds, relative permittivities, molar polarizations, excess isentropic compressibilities, and molar electrical susceptibilities were calculated, and the compositional dependence of each of the functions was expressed with a Redlich–Kister type equation. The variation of the Kirkwood correlation factor was determined over the complete composition range.

---

**KEY WORDS:** densities; deviation and excess functions; MMA + diethers; relative permittivities; sound speeds; viscosities.

## 1. INTRODUCTION

Keeping the importance of thermodynamic and thermophysical property data of binary and ternary systems involving acrylic esters, alcohols, and

---

<sup>1</sup> Department of Chemistry, Sardar Patel University, Vallabh Vidyanagar–388120, Gujarat, India.

<sup>2</sup> To whom correspondence should be addressed. E-mail: nvsastri\_ad1@sancharnet.in

hydrocarbons in mind, various excess or deviation functions derived from densities, sound speeds, viscosities, isentropic compressibilities, relative permittivities, and molar polarizations for the binary mixtures of alkyl methacrylates (methyl, ethyl, and butyl methacrylates) + *n*-hexane, or *n*-heptane, + carbon tetrachloride, + chloro- and + dichlorobenzenes [1–3], alkyl acrylates + 1-alcohols [4–6], methyl methacrylate + 1-alcohols/ alkoxy-ethanols [7, 8], methyl acrylate + *n*-alkanes [9], and methyl methacrylate + *n*-alkanes [10] and + aromatic hydrocarbons [11, 12] have been previously reported by us. Our analysis of the various functions revealed that both structure weakening and structure making interactions are present in these mixtures depending upon the nature of the second added components. For example, totally inert components such as *n*-alkanes predominantly disrupt the dipole-dipole forces in the acrylic esters, while aromatic hydrocarbons besides structure disruptions, could interact with acrylic esters with additional *n*--- $\pi$ , Cl---O, and Br---O specific contacts. Similarly, structure weakening in both alcohols as well as esters could take place in acrylic ester + alcohol mixtures depending upon the composition of one of the components. At the same time, formation of new hydrogen bonds could take place between –OH of alcohol and carbonyl group of ester species. A perusal of the literature showed that studies of the thermodynamic properties of acrylic esters + aliphatic ethers are very scarce. However, a few studies on binary systems of ethers + hydrocarbons [13–20, 21], + cyclohexane [21–23], and + 1-alcohols [24] have been reported.

Since the aliphatic ethers differ from *n*-alkanes by the presence of –O– in the place of a –CH<sub>2</sub>– group, the diethers such as diethyl ether (DEE), diisopropyl ether (DIPE), and dibutyl ether (DBE) can be considered structurally equivalent to *n*-pentane, *n*-heptane, and *n*-nonane in molecular architecture. Thus, when acrylic ester such as methyl methacrylate (MMA) is mixed with the above ethers, the MMA molecules can have opposing interactions with the nonpolar alkyl part and polar –O– part of the ethers. A recent attempt was also made by us [25] to carry out quantitative and qualitative analysis of excess molar volumes and excess molar enthalpies of MMA + DEE, + DIPE, and + DBE mixtures using Flory and Prigogine–Flory–Patterson (PFP) theories. In order to make available wide property data on binary systems of MMA + ethers, this paper reports primary properties such as densities, dynamic viscosities, sound speeds, and relative permittivities and various functions, namely, viscosity deviations, excess isentropic compressibilities, deviations in relative permittivity, and molar polarizations. An attempt was also made to apply semi-empirical equations for correlating the mixture viscosities and to predict the sound speeds using free length and collision factor theories as well as Nomoto and Junjie equations.

## 2. EXPERIMENTAL PROCEDURES

### 2.1. Materials

MMA was a laboratory reagent grade chemical obtained from Chiti-Chem, India. It was further washed with 25% (w/v) sodium hydroxide solution and then the alkali was washed out repeatedly with triple-distilled water treatment. The chemical was finally distilled in vacuum in a stream of nitrogen. DEE and DIPE were analytical reagent (AR) quality chemicals purchased from Chiti-Chem, India. DEE was further distilled over calcium chloride before use while DIPE was further washed with a solution of hydroxylamine hydrochloride for removal of peroxides and distilled twice. DBE was a Fluka product of AR quality and was used as such without any further purification. The purities of all the above chemicals determined by gas chromatography were found to be better than 99.5% on a molar basis. The experimental results for the density, viscosity, sound speeds, and relative permittivities of the pure liquids at  $T = 298.15$  and  $308.15$  K are compared with published data in Table I.

### 2.2. Methods

The binary mixtures were prepared by mixing the pure components in hermetically sealed glass vials. A set of eleven compositions was prepared for each system. The pure components were degassed by double distilling them just before mixing. The various physical properties of the prepared mixtures were measured on the same day.

Densities of the pure liquids and their mixtures were measured with a high precision vibrating tube digital densimeter (Anton Paar DMA 5000). The instrument has a built-in thermostat for maintaining desired temperatures in the range of 0 to 90°C. The repeatability of the temperature has been found to be  $\pm 0.002$  and  $\pm 0.003^\circ\text{C}$  for a given session and two different sessions, respectively. The accuracy in the temperature during the measurements however is  $\pm 0.01^\circ\text{C}$  because Pt 100 measuring sensors were used. The instrument was calibrated with air and four times distilled and freshly degassed water at  $T = 293.15$ ,  $313.15$ , and  $333.15$  K during each session. The repeatability in the densities for the distilled water and freshly distilled pure liquids and prepared binary mixtures have been found to be better than  $\pm 3.0 \times 10^{-6} \text{ g} \cdot \text{cm}^{-3}$ . We have estimated the accuracy in densities of the four pure liquids used in the study by comparing our data at different temperatures with the literature values, as listed in Table I. This comparison gave a mean absolute deviation of  $\pm 3.0 \times 10^{-5} \text{ g} \cdot \text{cm}^{-3}$ .

**Table I.** Densities ( $\rho$ ), Viscosities ( $\eta$ ), Sound Speeds ( $u$ ), and Relative Permittivities ( $\epsilon_r$ ) of Pure Components at 298.15 and 308.15 K

$T$ (K)	$\rho$ ( $\text{g} \cdot \text{cm}^{-3}$ )		$\eta$ ( $\text{mPa} \cdot \text{s}$ )		$u$ ( $\text{m} \cdot \text{s}^{-1}$ )		$\epsilon_r$		$n_D$		
	Exp.	Lit.	Exp.	Lit.	Exp.	Lit.	Exp.	Lit.			
MMA	298.15	0.937629	0.93766 [32]	0.585	0.584 [7]	1181	1182 [12]	6.534	6.533 [33]	1.4120	1.4120 [33]
	308.15	0.925743	0.9257 [7]	0.489	0.492 [7]	1153	1152 [12]	6.449	6.442 [11]	1.4068	
DEE	298.15	0.707866	0.70782 [33]	0.235		968		4.191	4.197 [33]	1.3495	1.3495 [33]
	308.15										
DIPE	298.15	0.718543	0.71854 [33]	0.380	0.379 [33]	998	999.16 [15]	3.880	3.88 [33]	1.3655	1.3655 [33]
	308.15	0.708204		0.285		962		3.732		1.3605	
DBE	298.15	0.764067	0.7641 [33]	0.641		1220		3.040		1.3969	1.3968 [33]
	308.15	0.755449		0.590		1179		2.964		1.3923	

Hence, the precision and uncertainty of the densities reported in the present work are  $\pm 3.0 \times 10^{-6}$  and  $\pm 3.0 \times 10^{-5} \text{ g} \cdot \text{cm}^{-3}$ , respectively.

The viscosities of pure and mixture components were obtained from the measured flow times using a suspended type Ubbelohde viscometer. The viscometer was suspended in a thermostatted water bath maintained to  $\pm 0.01^\circ\text{C}$ . Four sets of readings for the flow times were taken using a Racer stop watch that can register time to  $\pm 0.1 \text{ s}$ , and the arithmetic mean was taken for the calculation of the viscosity. The estimated uncertainty and precision in viscosity measurements were found to be the same, i.e.,  $\pm 0.002 \text{ mPa} \cdot \text{s}$ .

The sound speeds in pure liquids and in binary mixtures were measured using an ultrasonic interferometer (Mittal Enterprises, New Delhi, India) operating at a fixed frequency of 2 MHz. The measured speeds of sound have a precision of  $\pm 0.8 \text{ m} \cdot \text{s}^{-1}$  and an uncertainty better than  $\pm 1.2 \text{ m} \cdot \text{s}^{-1}$ .

The relative permittivities of the individual pure components and binary mixtures were calculated from the capacitance measurements with a universal dielectrometer, Type OH-301 of Radelkis, Hungary. The procedure used in the calibration of the dielectric cells was the same as described in detail elsewhere [26]. The measured relative permittivities have an estimated precision and uncertainty of  $\pm 0.001$  and  $\pm 0.004$ , respectively.

The temperature during the measurements of all the above properties was maintained accurate to  $\pm 0.01 \text{ K}$  by using a thermostatted INSREF (India) circulator (Model 020A). The binary mixtures were prepared by weighing, and the uncertainty in the mole fractions was estimated to be  $\pm 10^{-4}$ , while the maximum errors for  $V_m^E$ ,  $\delta\eta$ ,  $\delta u$ ,  $\kappa_s^E$ ,  $\delta\epsilon_r$ ,  $\chi_m^E$ , and  $\delta P_m$  were estimated to be better than  $0.001 \text{ cm}^3 \cdot \text{mol}^{-1}$ ,  $0.001 \text{ mPa} \cdot \text{s}$ ,  $0.3 \text{ m} \cdot \text{s}^{-1}$ ,  $1.3 \text{ TPa}^{-1}$ ,  $0.001$ ,  $0.001 \text{ mol} \cdot \text{cm}^{-3}$ , and  $0.3 \text{ cm}^3 \cdot \text{mol}^{-1}$ , respectively.

### 3. RESULTS AND DISCUSSION

#### 3.1. Densities ( $\rho$ ), Excess Molar Volumes ( $V_m^E$ ), Dynamic Viscosities ( $\eta$ ), and Viscosity Deviations ( $\delta\eta$ )

The measured densities and dynamic viscosities for MMA + DEE, +DIPE, and +DBE mixtures at different compositions and at  $T = 298.15$  and  $308.15 \text{ K}$  are given in Tables II and III, respectively. Excess molar volumes,  $V_m^E$  were calculated at  $T = 298.15$  and  $308.15 \text{ K}$  using the relation;

$$V_m^E / (\text{cm}^3 \cdot \text{mol}^{-1}) = \frac{x_1 M_1 + x_2 M_2}{\rho_{12}} - \left\{ \frac{x_1 M_1}{\rho_1} + \frac{x_2 M_2}{\rho_2} \right\} \quad (1)$$

Table II. Densities ( $\rho$ ) and Sound Speeds ( $u$ ) for MMA + Di-Ethers at 298.15 and 308.15 K

$x_1$	$\rho$ ( $\text{g} \cdot \text{cm}^{-3}$ )		$u$ ( $\text{m} \cdot \text{s}^{-1}$ )		$x_1$	$\rho$ ( $\text{g} \cdot \text{cm}^{-3}$ )		$u$ ( $\text{m} \cdot \text{s}^{-1}$ )		$x_1$	$\rho$ ( $\text{g} \cdot \text{cm}^{-3}$ )		$u$ ( $\text{m} \cdot \text{s}^{-1}$ )	
	298.15	308.15	298.15	308.15		298.15	308.15	298.15	308.15		298.15	308.15	298.15	308.15
	MMA(1)+DEE(2)					MMA(1)+DIPE(2)					MMA(1)+DBE(2)			
	T (K)					T (K)					T (K)			
0.0454	0.719520	979	0.0416	0.726106	0.715395	1004	969	0.0446	0.768791	0.760079	1219	1178		
0.1483	0.745218	1005	0.1479	0.745061	0.734243	1022	989	0.1479	0.779767	0.770999	1215	1175		
0.2490	0.769850	1031	0.2488	0.764073	0.753161	1040	1008	0.2442	0.791330	0.782369	1212	1173		
0.3495	0.793922	1055	0.3488	0.783897	0.772897	1059	1028	0.3388	0.804040	0.794784	1208	1171		
0.4486	0.817159	1078	0.4527	0.805528	0.794443	1078	1047	0.4495	0.820745	0.811045	1204	1169		
0.4908	0.826904	1087	0.4958	0.814811	0.803692	1086	1055	0.4924	0.827780	0.817888	1203	1168		
0.5479	0.839946	1099	0.5472	0.826118	0.814961	1095	1064	0.5489	0.837548	0.827391	1201	1167		
0.6504	0.862945	1119	0.6489	0.849250	0.838023	1113	1082	0.6504	0.856589	0.845940	1198	1165		
0.7501	0.884808	1137	0.7504	0.873344	0.862053	1130	1100	0.7489	0.876999	0.865877	1194	1163		
0.8488	0.905957	1154	0.8502	0.898016	0.886667	1149	1119	0.8501	0.900065	0.888493	1190	1160		
0.9470	0.926510	1171	0.9440	0.922090	0.910693	1168	1139	0.9428	0.923159	0.911233	1185	1156		

Table III. Viscosities ( $\eta$ ) and Deviations in Viscosities ( $\delta\eta$ ) for MMA + Di-Ethers at 298.15 and 308.15 K

$x_1$	298.15		308.15		298.15		308.15		$x_1$	298.15		308.15	
	$\eta$ (mPa·s)	$\delta\eta$ (mPa·s)	$\eta$ (mPa·s)	$x_1$	$\eta$ (mPa·s)	$\delta\eta$ (mPa·s)	$\eta$ (mPa·s)	$x_1$		$\eta$ (mPa·s)	$\delta\eta$ (mPa·s)		
	T (K)												
	MMA(1)+DEE(2)				MMA(1)+DIPE(2)				MMA(1)+DBE(2)				
0.0454	0.249	-0.002	0.0416	0.385	0.291	-0.003	-0.002	0.0446	0.633	0.581	-0.005	-0.005	308.15
0.1483	0.281	-0.007	0.1479	0.401	0.309	-0.010	-0.006	0.1479	0.616	0.561	-0.017	-0.014	
0.2490	0.314	-0.008	0.2488	0.417	0.326	-0.014	-0.010	0.2442	0.603	0.546	-0.024	-0.019	
0.3495	0.349	-0.008	0.3488	0.434	0.344	-0.017	-0.013	0.3388	0.593	0.532	-0.029	-0.024	
0.4486	0.385	-0.007	0.4527	0.453	0.364	-0.020	-0.013	0.4495	0.584	0.519	-0.032	-0.026	
0.4908	0.400	-0.007	0.4958	0.461	0.372	-0.021	-0.014	0.4924	0.581	0.515	-0.032	-0.025	
0.5479	0.421	-0.006	0.5472	0.472	0.383	-0.020	-0.014	0.5489	0.579	0.510	-0.031	-0.024	
0.6504	0.459	-0.003	0.6489	0.493	0.404	-0.020	-0.013	0.6504	0.576	0.502	-0.028	-0.022	
0.7501	0.496	-0.002	0.7504	0.517	0.427	-0.017	-0.011	0.7489	0.575	0.496	-0.024	-0.018	
0.8488	0.532	-0.001	0.8502	0.542	0.451	-0.012	-0.008	0.8501	0.577	0.492	-0.016	-0.012	
0.9470	0.567	0.001	0.9440	0.569	0.474	-0.004	-0.004	0.9428	0.581	0.490	-0.008	-0.005	

The compositional variation of  $V_m^E$  was mathematically represented through an equation of the type,

$$A^E = x_1(1-x_1) \sum_{i=0}^{i=n} a_i(2x_1-1)^i \quad (2)$$

where  $A^E = V_m^E$ ,  $a_i$  are the fitting coefficients, and  $x_1$  is the MMA mole fraction. The values of  $a_i$  were estimated by a least-squares method using multiple regression analysis. The summary of  $a_i$  and  $\sigma$ , the standard deviations between experimental and fitted  $V_m^E$  values, is given in Table IX. The compositional variation of  $\eta$  for the three mixtures is shown in Fig. 1a. It can be seen from the figure that  $\eta$  values vary nonlinearly with  $x_1$  for the three mixtures. The  $\eta$  values are found to increase continuously for MMA+DEE and +DIPE systems while a rectilinear decreasing trend was observed for the MMA+DBE system. The nonlinearity observed in  $\eta$  versus  $x_1$  profiles, in general, indicates that considerable deviations from ideal mixing are present in these mixtures.

### 3.1.1. Correlation of Mixture Viscosities

The compositional variations of dynamic viscosities, kinematic viscosities,  $\nu$  and viscosity ratios of MMA+diether systems were further tested

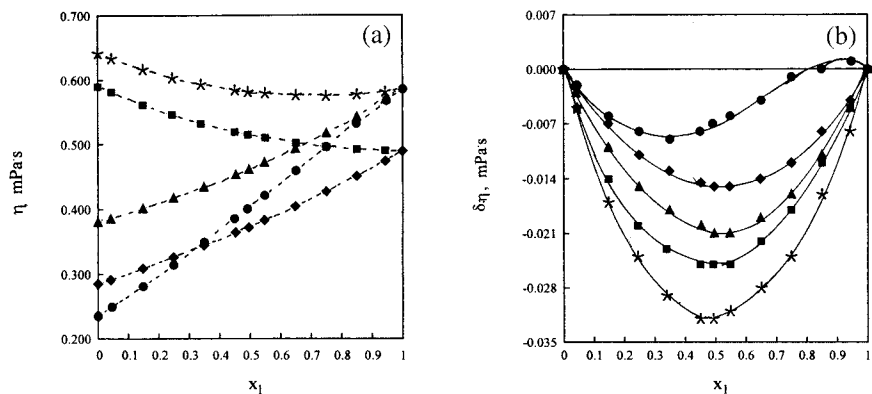


**Fig. 1.** (a) Experimental dynamic viscosities,  $\eta$  and (b) deviations in viscosities,  $\delta\eta$  as a function of MMA mole fraction for MMA+di-ethers: ●, DEE; ▲, DIPE; and \*, DBE at  $T = 298.15$  K and ◆, DIPE; and ■, DBE at  $T = 308.15$  K. (---) in part a indicates the Grunberg-Nissan equation correlated values.



below using Grunberg–Nissan (GN), McAllister (Mc) and Auslander (A) equations:

$$\ln \eta_{12} = x_1 \ln \eta_1 + x_2 \ln \eta_2 + x_1 x_2 G_{12} \quad (3)$$

$$\begin{aligned} \ln v_{12} = & x_1^3 \ln v_1 + 3x_1^2 x_2 \ln M_{12} + 3x_1 x_2^2 \ln M_{21} + x_2^3 \ln v_2 - \ln \left( x_1 + \frac{x_2 M_2}{M_1} \right) \\ & + 3x_1^2 x_2 \ln \left( \frac{2}{3} + \frac{M_2}{3M_1} \right) + 3x_1 x_2^2 \ln \left( \frac{1}{3} + \frac{2M_2}{3M_1} \right) + x_2^3 \ln \left( \frac{M_2}{M_1} \right) \end{aligned} \quad (4)$$

$$x_1(x_1 + B_{12}x_2)(\eta_{12} - \eta_1) + A_{21}x_2(B_{21}x_1 + x_2)(\eta_{12} - \eta_2) = 0 \quad (5)$$

These equations are particularly selected because the characteristic constant parameter  $G_{12}$  of Eq. (3) allows for positive and negative deviations from the additivity rule. Equation (4) is based on the Eyring theory for absolute reaction rates with a three-body interaction model, and Eq. (5) involves three parameters. The terms  $G_{12}$ ,  $M_{12}$ ,  $M_{21}$ ,  $B_{12}$ ,  $A_{21}$ , and  $B_{21}$  in the above equations have been considered as adjustable parameters and were estimated by a nonlinear regression analysis based on a least-squares method. The values of the individual parameters along with the standard deviations ( $\sigma$ ) between the experimental and correlated values are given in Table IV. A perusal of  $\sigma$  values shows that both GN and McAllister equations correlate the viscosities adequately but the predicted viscosity ratios from the Auslander equation had  $\sigma$  values ranging from 0.012 to 0.125. Thus the GN equation with one single adjustable parameter provides a better fit and thus is superior in correlating the viscosities in the present mixtures.

**Table IV.** Adjustable Parameters and Standard Deviations ( $\sigma$ ) (in mPa·s) for the Correlation of Mixture Viscosities for MMA + Di-Ethers at 298.15 and 308.15 K

	$G_{12}$	$\sigma$	$M_{12}$	$M_{21}$	$\sigma$	$A_{21}$	$B_{21}$	$B_{12}$	$\sigma$
$T = 298.15 \text{ K}$									
MMA +									
DEE	0.338	0.001	0.552	0.455	0.002	1.128	0.953	0.984	0.043
DIPE	-0.081	0.001	0.578	0.549	0.001	0.235	5.681	0.125	0.122
DBE	-0.211	0.001	0.662	0.731	0.001	0.820	-1.338	2.701	0.012
$T = 308.15 \text{ K}$									
MMA +									
DEE									
DIPE	-0.002	0.001	0.485	0.446	0.001	0.406	2.828	0.275	0.125
DBE	-0.175	0.001	0.588	0.665	0.001	0.311	0.734	0.628	0.023

### 3.1.2. Viscosity Deviations ( $\delta\eta$ )

The  $\delta\eta$  values were calculated using the relation,

$$\delta\eta/(\text{mPa}\cdot\text{s}) = \eta_{12} - (x_1\eta_1 + x_2\eta_2) \quad (6)$$

where the subscripts 1, 2, and 12 refer to pure MMA, ether, and the binary mixture, respectively. The compositional variation of  $\delta\eta$  was mathematically expressed by using Eq. (2), where  $A^E = \delta\eta$ . The standard deviations,  $\sigma$ , were calculated by using the equation,

$$\sigma = \{\Sigma(A_{\text{exp}}^E - A_{\text{fit}}^E)^2/(n-p)\}^{1/2} \quad (7)$$

where  $A_{\text{exp}}^E$  and  $A_{\text{fit}}^E$  are the experimental and fitted values of the respective function. A summary of the analysis is given in Table IX. The  $\delta\eta$  values are plotted as a function of  $x_1$  in part b of Fig. 1. The  $\delta\eta$  values are all negative for MMA + DIPE and +DBE at  $T = 298.15$  and  $308.15$  K and showed asymmetric sigmoidal behavior with small negative values up to  $x_1 \approx 0.8$  before approaching zero beyond  $x_1 \approx 0.8$ . The increase in temperature from 298.15 to 308.15 K resulted in less negative  $\delta\eta$  values. Otherwise,  $\delta\eta$  values become more negative with the lengthening of the alkyl chain in ethers. The small negative  $\delta\eta$  values indicate the presence of weak but specific dipole-dipole forces between MMA and ethers. Such contributions are expected to be more prevalent in MMA + DEE than in MMA + DBE systems.

## 3.2. Sound Speeds ( $u$ ), Deviation in Sound Speeds ( $\delta u$ ), and Excess Isentropic Compressibilities ( $\kappa_s^E$ )

The experimental sound speeds,  $u$  are listed in Table II. The compositional dependence of  $u$  in the three binary mixtures is depicted in part a of Fig. 2. The  $u$  values were also calculated from the approaches of free length theory (FLT) and collision factor theory (CFT) and using Nomoto and Junjie equations. The pertinent equations used in the calculations are summarized below:

### 3.2.1. Free Length Theory (FLT)

The intermolecular free length ( $L_f$ ) is defined by the relation,

$$L_f = 2V_a/Y \quad (8)$$

where  $V_a$  = available volume and is related to molar volume,  $V_m$  and volume at absolute zero,  $V_0$  through

$$V_a = V_m - V_0 \quad (9)$$

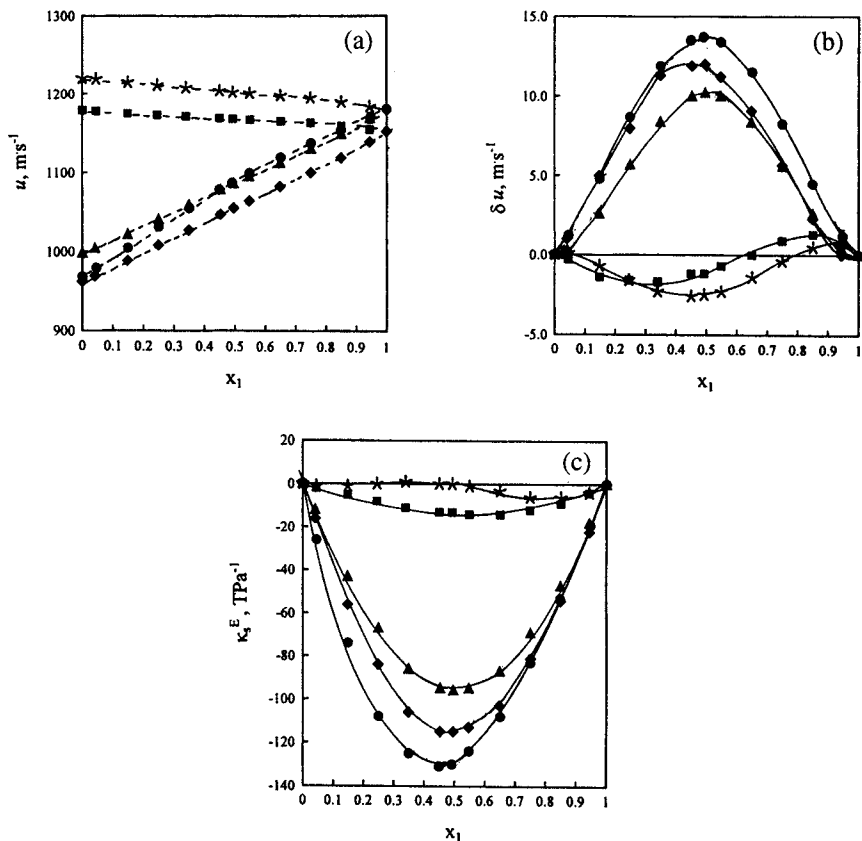


Fig. 2. (a) Experimental sound speeds,  $u$ , (b) deviation in sound speeds,  $\delta u$  and (c) excess isentropic compressibilities ( $\kappa_s^E$ ) as a function of MMA mole fraction for MMA + di-ethers. (Symbols same as those in Fig. 1.) (---) in part a indicates the CFT predicted values.

and  $Y$  is the surface area per mole. The value of  $Y$  is calculated from  $Y = (36\pi N_A V_0^2)^{1/3}$  where  $N_A =$  Avogadro's number. The following relation was set up between the isentropic compressibility and free length of several pure liquids [27]:

$$\log \kappa_s = \log k + p \log L_f \quad (10)$$

where  $k$  and  $p$  are temperature dependent coefficients. As already defined  $\kappa_s = 1/(u^2 \rho)$ , and by substituting it in the above equation we obtain

$$\log(1/(u^2 \rho)) = \log k + p \log L_f \quad (11)$$

The concept of free length is extended to the case of liquid mixtures [29] and is defined as

$$L_{f,\text{mix}} = 2[V_m - x_1V_0^1 + x_2V_0^2]/(x_1Y_1 + x_2Y_2) \quad (12)$$

where  $V_m$  is the molar volume of the mixture and  $V_0$  is the molar volume at absolute zero for the pure components and is calculated by the formula,

$$V_{0,i} = V_m(1 - (T/T_{c,i}))^{0.3} \quad (13)$$

where  $T_{c,i}$  is the critical temperature of the respective  $i$ th pure component. The free length value as estimated by Eq. (11) represents the ideal state in which association effects are neglected because the constants  $k$  and  $p$  that appear in that equation were evaluated from a linear relation between the isentropic compressibilities and free lengths for 54 non-associating liquids [27]. So by calculating  $L_{f,\text{mix}}$  from Eq. (12) and using the values of the constants,  $k$  and  $p$  for Eq. (11) ( $k=7.274$  and  $7.629$ ;  $p=2.106$  and  $2.148$  at  $T=298.15$  and  $308.15$  K, respectively), the sound speeds were calculated.

### 3.2.2. Collision Factor Theory (CFT)

This theory proposes the following equations for calculating the speed of sound in pure liquids,

$$u = u_\infty S r_j = u_\infty S B / V_m \quad (14)$$

where  $u_\infty = 1600 \text{ m} \cdot \text{s}^{-1}$ ;  $S$  = collision factor; and  $r_j$  = spacing filling factor equal to  $B/V_m$ , where  $B$  = actual volume of the molecule per mole. This concept was extended to binary liquid mixtures [29],

$$v_{\text{mix}} = v_\infty [x_1 S_1 + x_2 S_2] (x_1 B_1 + x_2 B_2) / V_m \quad (15)$$

The actual volumes of the molecule per mole ( $B_1$  and  $B_2$ ) for the pure components were calculated using the relation,  $B_i = 4\pi r_m^3 N_A / 3$  where  $r_m$  stands for the molecular radius and  $N_A$  is Avogadro's number. The molecular radius,  $r_m$ , was obtained from the expressions,

$$r_m = \alpha [1 - \beta \{ (1 + (1/3\beta))^{1/2} - 1 \}]^{1/3} \quad (16)$$

$$\text{where } \alpha = (3V_m / (16\pi N))^{1/3} \quad (17)$$

and

$$\beta = (\gamma R T / (M u^2)) \quad (18)$$

$\gamma$ ,  $R$ , and  $M$  stand for the specific heat ratio, gas constant, and the molecular weight of each pure component.

### 3.2.3. Junjie ( $u_j$ ) Equation

The Junjie equation [30] has the form,

$$u_j = \left\{ (x_1 M_1 / \rho_1) + (x_2 M_2 / \rho_2) \right\} / \left\{ (x_1 M_1 + x_2 M_2)^{1/2} \right. \\ \left. \times [(x_1 M_1 / \rho_1 v_1^2) + (x_2 M_2 / \rho_2 v_2^2)^{1/2}] \right\} \quad (19)$$

where  $x_i$ ,  $M_i$ ,  $\rho_i$ , and  $v_i$  are the mole fraction, molar mass, density, and sound speed, respectively, for component  $i$ . The various calculated physico-chemical properties that appear in the above equations are listed in Table V.

### 3.2.4. Nomoto ( $u_N$ ) Equation

Theoretical values of speed of sound ( $u_N$ ) can also be obtained using the Nomoto equation [31],

$$u_N = \left\{ (x_1 R_1 + x_2 R_2) / (x_1 V_{m,1} + x_2 V_{m,2}) \right\} \quad (20)$$

where  $V_{m,i}$  is the molar volume of component  $i$  and  $R$  is Wada's constant and was calculated from  $R_i = u_i^{1/3} V_{m,i}$ , where  $u_i$  is the sound speed of  $i$ th component.

### 3.2.5. Comparisons

Comparisons of the predicted and experimental  $u$  values along with the percentage standard deviations ( $\sigma\%$ ) between experimental and predicted values are given in Table VI. It is found that the CFT approach predicted the  $u$  values with standard deviations ranging from 0.3 to 0.6%. The FLT approach and Nomoto equation yielded  $u$  values with larger deviations than the CFT approach, ranging from 0.1 to 9.3%. However, the Junjie equation has been found to yield  $u$  values with very large deviations (compared to the other three approaches) ranging from 10.2 to 11.3%.

### 3.2.6. Deviation in Sound Speeds ( $\delta u$ ) and Excess Isentropic Compressibilities ( $\kappa_s^E$ )

The functions  $\delta u$  and  $\kappa_s^E$  were calculated using the relations:

$$\delta u / (\text{m} \cdot \text{s}^{-1}) = u_{12} - (\phi_1 u_1 + \phi_2 u_2) \quad (21)$$

$$\kappa_s^E / (\text{TPa}^{-1}) = \kappa_s - \kappa_s^{\text{id}} \quad (22)$$

Table V. Physico-Chemical Properties for Pure Components at 298.15 and 308.15 K<sup>a</sup>

$V_m$ ( $\text{cm}^3 \cdot \text{mol}^{-1}$ )	$V_0$ ( $\text{cm}^3 \cdot \text{mol}^{-1}$ )	$V_a$ ( $\text{cm}^3 \cdot \text{mol}^{-1}$ )	$L_f$ ( $\text{\AA}$ )	$Y$	$S$	$B$ ( $\text{cm}^3 \cdot \text{mol}^{-1}$ )	$r_j$ ( $\text{\AA}$ )	$C_p$ ( $\text{J} \cdot \text{K}^{-1} \cdot \text{mol}^{-1}$ )	$\alpha$ ( $\text{k} \cdot \text{K}^{-1}$ )
$T = 298.15 \text{ K}$									
MMA	106.780	84.408	0.590	75.87	2.965	26.580	1.412	191.1	1.236
DEE	104.712	76.492	0.767	73.58	2.434	26.024	1.350	172.5	1.661
DIPE	142.199	106.624	0.775	91.82	2.507	35.376	1.366	216.1	1.446
DBE	170.443	137.483	0.606	108.77	3.061	42.460	1.397	278.2	1.142
$T = 308.15 \text{ K}$									
MMA	108.151		0.626		2.897	26.907	1.407	198.2	1.263
DEE									
DIPE	144.275		0.820		2.419	35.866	1.361	221.6	1.488
DBE	172.388		0.642		2.960	42.922	1.392	292.0	1.163

<sup>a</sup>  $V_m$  = molar volume,  $V_0$  = molar volume at absolute zero,  $V_a$  = available volume,  $L_f$  = free length,  $Y$  = surface area,  $S$  = collision factor,  $B$  = actual volume per mole,  $r_j$  = molecular radius,  $C_p$  = isobaric heat capacity,  $\alpha$  = isobaric thermal expansion coefficient.

Table VI. Predicted Sound Speeds (in  $\text{m} \cdot \text{s}^{-1}$ ) for MMA + Di-Ethers at 298.15 and 308.15 K

$x_1$	$u_{\text{FLT}}$	$u_{\text{CFT}}$	$u_{\text{N}}$	$u_{\text{FLT}}$	$u_{\text{CFT}}$	$u_{\text{N}}$
$T = 298.15 \text{ K}$			$T = 308.15 \text{ K}$			
MMA(1)+DEE(2)						
0.0454	971	979	977			
0.1483	989	1006	998			
0.2490	1005	1026	1019			
0.3495	1021	1049	1040			
0.4486	1035	1070	1061			
0.4908	1041	1079	1070			
0.5479	1049	1091	1082			
0.6504	1063	1112	1105			
0.7501	1075	1133	1126			
0.8488	1086	1152	1148			
0.9470	1096	1171	1169			
$\sigma\%$	3.5	0.5	1.2			
MMA(1)+DIPE(2)						
0.0416	952	1007	1003	886	970	968
0.1479	965	1027	1018	899	992	983
0.2488	979	1046	1033	912	1012	998
0.3488	994	1065	1048	927	1032	1014
0.4527	1011	1085	1066	943	1052	1032
0.4958	1018	1093	1073	950	1061	1040
0.5472	1026	1103	1082	958	1071	1050
0.6489	1044	1121	1102	974	1090	1070
0.7504	1061	1139	1123	991	1109	1092
0.8502	1076	1156	1145	1007	1127	1115
0.9440	1091	1171	1167	1021	1143	1138
$\sigma\%$	6.4	0.63	0.9	9.3	0.6	1.0
MMA(1)+DBE(2)						
0.0446	1183	1218	1219	1106	1178	1178
0.1479	1168	1212	1216	1093	1173	1176
0.2442	1157	1208	1213	1083	1170	1174
0.3388	1149	1204	1210	1075	1167	1173
0.4495	1142	1200	1207	1067	1164	1170
0.4924	1140	1198	1205	1064	1163	1169
0.5489	1137	1196	1203	1062	1162	1168
0.6504	1133	1193	1199	1057	1160	1165
0.7489	1129	1191	1195	1052	1159	1162
0.8501	1122	1188	1189	1046	1157	1159
0.9428	1114	1184	1184	1039	1155	1155
$\sigma\%$	5.3	0.3	0.1	9.1	0.4	1.0

where  $\kappa_s$  is the isentropic compressibility and was calculated using the Laplace equation, i.e.,  $\kappa_s = 1/(u^2\rho)$  and  $\kappa_s^{\text{id}}$  was calculated from the relation,

$$\kappa_s^{\text{id}} = \sum_{i=1}^2 \phi_i [\kappa_{s,i} + TV_{m,i}(\alpha_i^2)/C_{p,i}] - \left\{ T \left( \sum_{i=1}^2 x_i V_{m,i} \right) \left( \sum_{i=1}^2 \phi_i \alpha_i \right)^2 / \sum_{i=1}^2 x_i C_{p,i} \right\} \quad (23)$$

where  $\phi_i$  is the ideal state volume fraction and is defined by the relation,

$$\phi_i = x_i V_{m,i} / \left( \sum_{i=1}^2 x_i V_{m,i} \right) \quad (24)$$

The data for  $\delta u$  and  $\kappa_s^E$  for the three mixtures as a function of MMA mole composition are given in Table VII. The  $\delta u$  and  $\kappa_s^E$  are also smoothed using Eq. (2). The values of the coefficients  $a_i$  and  $\sigma$  obtained from the analysis are listed in Table IX. The graphical variation of  $\delta u$  and  $\kappa_s^E$  with the MMA mole fraction is shown in parts b and c of Fig. 2. It can be seen from Fig. 2b that the  $\delta u$  values for MMA + DEE and + DIPE are too large and positive. A systematic decrease in the magnitude of  $\delta u$  was observed when DEE is replaced by DIPE and DBE. In fact, in MMA + DBE mixtures, the  $\delta u$  values become small and negative for most of the range except for slight positive values in the MMA-rich region. As  $\kappa_s$  is inversely proportional to  $u$ , the trend in  $\kappa_s^E$  values (part c of Fig. 2) has been found to be opposite to that observed in  $\delta u$  versus  $x_1$  profiles. Except for MMA + DBE at  $T = 298.15$  K,  $\kappa_s^E$  values are negative over the complete composition range for the three mixtures. The absolute magnitude has been found to increase by a factor of about 12 in MMA + DEE mixtures at  $T = 298.15$  K as compared to MMA + DBE systems. The large and negative  $\kappa_s^E$  in MMA + DEE systems is an indication of the presence of weak but structure-making specific dipole-dipole interactions between short alkyl-chained DEE and MMA molecules. As the alkyl chain length is doubled for DBE, the increased nonpolar fraction in the molecule dilutes the etheric fraction, and hence, one would expect more dispersing structure weakening interactions resulting in highly diminished negative  $\kappa_s^E$  values.

### 3.3. Relative Permittivities ( $\epsilon_r$ ) and Related Functions

Relative permittivities ( $\epsilon_r$ ) were combined with densities to calculate the molar electrical susceptibilities,  $\chi_m$  and molar polarizations,  $P_m$ . Then



**Table VII.** Deviations in Sound Speed ( $\delta u$ ) and Excess Isentropic Compressibilities ( $\kappa_s^E$ ) for MMA + Di-Ethers at 298.15 and 308.15 K

$x_1$	$\delta u$ ( $\text{m} \cdot \text{s}^{-1}$ )		$\kappa_s^E$ ( $\text{TPa}^{-1}$ )		$x_1$	$\delta u$ ( $\text{m} \cdot \text{s}^{-1}$ )		$\kappa_s^E$ ( $\text{TPa}^{-1}$ )	
$T$ (K)									
298.15					308.15				
MMA(1)+DEE(2)					MMA(1)+DIPE(2)				
0.0454	1.1		-26		0.0416	0.2	1.0	-12	-16
0.1483	5.0		-74		0.1479	2.9	5.0	-43	-56
0.2490	9.2		-108		0.2488	5.5	8.0	-67	-84
0.3495	11.6		-125		0.3488	8.5	11.3	-86	-106
0.4486	13.4		-131		0.4527	9.9	11.9	-95	-115
0.4908	13.4		-130		0.4958	10.3	12.0	-96	-115
0.5479	13.3		-124		0.5472	9.9	11.2	-95	-113
0.6504	11.5		-108		0.6489	8.6	9.1	-87	-103
0.7501	8.5		-83		0.7504	5.2	5.7	-69	-81
0.8488	4.7		-53		0.8502	2.8	2.3	-47	-54
0.9470	1.1		-19		0.9440	0.4	0.0	-18	-22
MMA(1)+DBE(2)									
0.0446	0.1	-0.3	-1	-2					
0.1479	-1.2	-1.4	1	-5					
0.2442	-1.4	-1.6	0	-8					
0.3388	-2.5	-1.7	1	-11					
0.4495	-2.8	-1.2	1	-13					
0.4924	-2.3	-1.2	-1	-13					
0.5489	-2.1	-0.7	-2	-14					
0.6504	-1.0	0.0	-5	-14					
0.7489	-0.6	0.9	-5	-12					
0.8501	0.4	1.3	-5	-9					
0.9428	0.6	0.7	-4	-4					

the deviations in relative permittivities,  $\delta \varepsilon_r$ , excess molar electrical susceptibilities,  $\chi_m^E$ , and deviations in molar polarizations,  $\delta P_m$ , were calculated using the following relation:

$$\delta \varepsilon_r = \varepsilon_{r,12} - \sum \phi_i \varepsilon_{r,i} \quad (25)$$

where  $\phi_i$  is the ideal state volume fraction of pure component  $i$  and  $\varepsilon_{r,i}$  is the relative permittivity of pure component  $i$ .

$$\chi_m^E (\text{cm}^{-3} \cdot \text{mol}) = \chi_{12} - (x_1 \chi_1 + x_2 \chi_2) \quad (26)$$

where  $\chi_{m,i}$  was calculated using the relations,  $\chi_i = ((\epsilon_{r,i} - 1)/V_{m,i})$  and  $\chi_{12} = ((\epsilon_{r,12} - 1)/V_{m,12})$ , where  $V_{m,i}$  is the molar volume of component  $i$ .

$$\delta P_m (\text{cm}^3 \cdot \text{mol}^{-1}) = P_{12} - (x_1 P_1 + x_2 P_2) \quad (27)$$

$P_i$  was calculated from  $(\epsilon_{r,i} - 1) (2\epsilon_{r,i} + 1) V_{m,i} / (9\epsilon_{r,i})$  and  $P_{12} = ((\epsilon_{r,12} - 1) (2\epsilon_{r,12} + 1) / (9\epsilon_{r,12})) ((x_1 M_1 + x_2 M_2) / \rho_{12})$  for the pure components and mixture, respectively. The results for  $\epsilon_r$ ,  $\delta\epsilon_r$ , and  $\delta P_m$  are given in Table VIII. All these functions were, as usual, tested for their mathematical consistency using Eq. (2). The values of the coefficients,  $a_i$ , along with  $\sigma$  values for each of the functions are summarized in Table IX.

The variations of  $\delta\epsilon_r$ ,  $\chi_m^E$ , and  $\delta P_m$  as a function of MMA mole fraction for all three binary mixtures are shown in parts a to c of Fig. 3.  $\delta\epsilon_r$ ,  $\chi_m^E$  values are found to be large and negative for MMA + DBE mixtures at  $T = 298.15$  and  $308.15$  K. But the same functions become less negative (for  $\chi_m^E$  of MMA + DIPE) and even positive for MMA + DEE and MMA + DIPE ( $\delta\epsilon_r$  values). The negative  $\delta\epsilon_r$  and  $\chi_m^E$  values for the MMA + DBE mixture clearly indicate that upon mixing of these components, the dielectric changes are significant. Molar electrical susceptibility values indicate the extent of perturbation in the dipole arrangement in the applied electrical field. Negative  $\chi_m^E$  values arise mainly because of loss of dipolar association both in MMA and DBE species upon mixing. These disruptions might have been equally compensated by the formation of new associates between MMA and DEE molecules due to dipole-dipole structure making interactions and, hence, this mixture has mostly positive  $\delta\epsilon_r$  and  $\chi_m^E$  values. The  $\delta P_m$  versus  $x_1$  profiles followed the qualitative trend as observed in  $\delta\epsilon_r$  versus  $x_1$  curves. The observed large and negative  $\delta P_m$  values support our earlier conclusion that in MMA + DBE systems, the relatively longer nonpolar alkyl chain induces more dispersion interactions with MMA molecules.

The differences in the overall interactions in MMA and DEE mixtures, vis-a-vis in MMA and DIPE and DEE systems, became distinctly clear from the monitoring of variations in  $g_K$ , the dielectric correlation parameter, across the MMA mole fraction for the three mixtures at  $T = 298.15$  K. The  $g_K$  value was calculated by using the relation,

$$g_K = \left\{ \frac{(\epsilon_{r,12} - \epsilon_\alpha)(2\epsilon_{r,12} + \epsilon_\alpha)}{\epsilon_{r,12}(\epsilon_\alpha + 2)^2} \right\} \left\{ \frac{9kT}{4\pi N(x_1 \mu_1 + x_2 \mu_2)^2} \right\} V_{m,12} \quad (28)$$

where  $k$  and  $\mu_i$  are Boltzmann's constant and the dipole moment of component  $i$ .  $\epsilon_\alpha$  is equal to  $1.1 n_D^2$ , where  $n_D$  is the refractive index. The  $g_K$  value gives a qualitative measure of the orientation of neighboring dipoles in bulk structures of pure liquid or complex fluid systems. A value of unity

**Table VIII.** Relative Permittivities ( $\epsilon_r$ ), Relative Permittivity Deviations ( $\delta\epsilon_r$ ), Excess Molar Electrical Susceptibilities ( $\chi_m^E$ ), and Deviations in Molar Polarizations ( $\delta P_m$ ) for MMA + Di-Ethers at 298.15 and 308.15 K

$x_1$	$\epsilon_r$		$\delta\epsilon_r$		$\chi_m^E$ (mol·cm <sup>-3</sup> )		$\delta P_m$ (cm <sup>3</sup> ·mol <sup>-1</sup> )	
	298.15	308.15	298.15	308.15	298.15	308.15	298.15	308.15
<i>T</i> (K)								
MMA(1)+DEE(2)								
0.0473	4.317		0.018		0.000		0.3	
0.1507	4.610		0.067		0.001		1.3	
0.2509	4.896		0.113		0.001		2.3	
0.3512	5.168		0.148		0.002		3.0	
0.4570	5.418		0.165		0.002		3.3	
0.4987	5.518		0.166		0.002		3.3	
0.5442	5.647		0.161		0.002		3.2	
0.6512	5.862		0.137		0.002		2.7	
0.7510	6.055		0.098		0.001		1.9	
0.8528	6.238		0.052		0.001		0.9	
0.9438	6.426		0.014		0.000		0.2	
MMA(1)+DIPE(2)								
0.0416	3.970	3.830	0.006	0.012	-0.001	0.000	0.1	0.4
0.1479	4.210	4.090	0.024	0.045	-0.002	-0.001	0.7	1.4
0.2488	4.446	4.344	0.039	0.073	-0.002	-0.002	1.0	2.1
0.3488	4.687	4.603	0.047	0.094	-0.003	-0.003	1.1	2.6
0.4527	4.975	4.878	0.048	0.106	-0.003	-0.003	1.1	2.8
0.4958	5.053	4.994	0.045	0.109	-0.003	-0.003	1.0	2.9
0.5472	5.186	5.134	0.041	0.108	-0.003	-0.003	0.9	2.8
0.6489	5.449	5.408	0.028	0.099	-0.003	-0.003	0.4	2.3
0.7504	5.727	5.689	0.013	0.081	-0.003	-0.002	-0.1	1.6
0.8502	6.029	5.985	-0.001	0.053	-0.002	-0.002	-0.2	1.1
0.9440	6.335	6.271	-0.005	0.021	-0.001	-0.001	-0.2	0.4
MMA(1)+DBE(2)								
0.0446	3.122	3.046	-0.017	-0.017	-0.001	-0.001	-0.5	-0.5
0.1479	3.289	3.224	-0.094	-0.082	-0.004	-0.004	-3.1	-2.7
0.2442	3.449	3.401	-0.179	-0.151	-0.006	-0.006	-5.8	-4.8
0.3388	3.641	3.611	-0.248	-0.201	-0.008	-0.007	-7.7	-6.2
0.4495	3.937	3.921	-0.286	-0.224	-0.009	-0.009	-8.5	-6.5
0.4924	4.076	4.062	-0.285	-0.221	-0.010	-0.009	-8.3	-6.3
0.5489	4.281	4.268	-0.271	-0.206	-0.010	-0.009	-7.6	-5.6
0.6504	4.709	4.689	-0.212	-0.152	-0.009	-0.009	-5.6	-3.9
0.7489	5.188	5.154	-0.128	-0.082	-0.008	-0.007	-3.2	-1.8
0.8501	5.726	5.670	-0.041	-0.015	-0.005	-0.005	-0.9	-0.1
0.9428	6.231	6.156	0.005	0.014	-0.002	-0.002	0.1	0.4

**Table IX.** Values of Coefficients, ( $a_i$ ) and Standard Deviations, ( $\sigma$ ) for Representation of Various Excess and Deviation Functions for Binary Mixtures of MMA + Di-Ethers at 298.15 and 308.15 K

	T = 298.15 K					T = 308.15 K						
	$a_0$	$a_1$	$a_2$	$\sigma$	$a_0$	$a_1$	$a_2$	$\sigma$	$a_0$	$a_1$	$a_2$	$\sigma$
<b>MMA + DEE</b>												
$V_m^E$ ( $\text{cm}^3 \cdot \text{mol}^{-1}$ )	-2.628	0.567	-0.035	0.001								
$\delta\eta$ (mPa·s)	-0.028	0.035	0.012	0.001								
$\delta u$ ( $\text{m} \cdot \text{s}^{-1}$ )	54.8	-2.5	-36.8	0.3								
$\kappa_s^E$ (TPa $^{-1}$ )	516	125	34	0.5								
$\delta\epsilon_T$	0.662	-0.085	-0.390	0.001								
$\chi_m^E$ ( $\text{cm}^{-3} \cdot \text{mol}$ )	0.009	0.000	-0.009	0.001								
$\delta P_m$ ( $\text{cm}^3 \cdot \text{mol}^{-1}$ )	13.4	-2.0	-9.6	0.1								
<b>DIPE</b>												
$V_m^E$ ( $\text{cm}^3 \cdot \text{mol}^{-1}$ )	-1.982	0.056	0.197	0.001	-2.015	-0.546	0.242	0.001				
$\delta\eta$ (mPa·s)	-0.083	-0.007	0.004	0.001	-0.055	-0.011	-0.008	0.001				
$\delta u$ ( $\text{m} \cdot \text{s}^{-1}$ )	40.7	-0.4	-41.3	0.2	47.9	-14.9	-42.5	0.2				
$\kappa_s^E$ (TPa $^{-1}$ )	-386	-17	75	0.8	-461	5	64	1.2				
$\delta\epsilon_T$	0.182	-0.141	-0.189	0.001	0.435	0.045	-0.102	0.001				
$\chi_m^E$ ( $\text{cm}^{-3} \cdot \text{mol}$ )	-0.011	0.001	-0.012	0.001	-0.013	-0.007	0.003	0.001				
$\delta P_m$ ( $\text{cm}^3 \cdot \text{mol}^{-1}$ )	4.0	-4.5	-5.4	0.1	11.2	-1.8	-3.0	0.1				
<b>DBE</b>												
$V_m^E$ ( $\text{cm}^3 \cdot \text{mol}^{-1}$ )	1.324	-1.931	-1.524	0.001	1.404	-1.476	-1.300	0.001				
$\delta\eta$ (mPa·s)	-0.127	-0.005	-0.007	0.001	-0.100	0.012	-0.005	0.001				
$\delta u$ ( $\text{m} \cdot \text{s}^{-1}$ )	-10.1	6.7	19.2	0.3	-4.3	12.9	8.9	0.2				
$\kappa_s^E$ (TPa $^{-1}$ )	-1	-31	-52	1.3	-53	-18	-7	0.6				
$\delta\epsilon_T$	-1.136	0.306	1.223	0.001	-0.878	0.389	1.005	0.001				
$\chi_m^E$ ( $\text{cm}^{-3} \cdot \text{mol}$ )	-0.039	-0.007	0.010	0.001	-0.034	-0.009	0.005	0.001				
$\delta P_m$ ( $\text{cm}^3 \cdot \text{mol}^{-1}$ )	-32.9	11.2	34.8	0.3	-24.9	13.6	28.3	0.2				

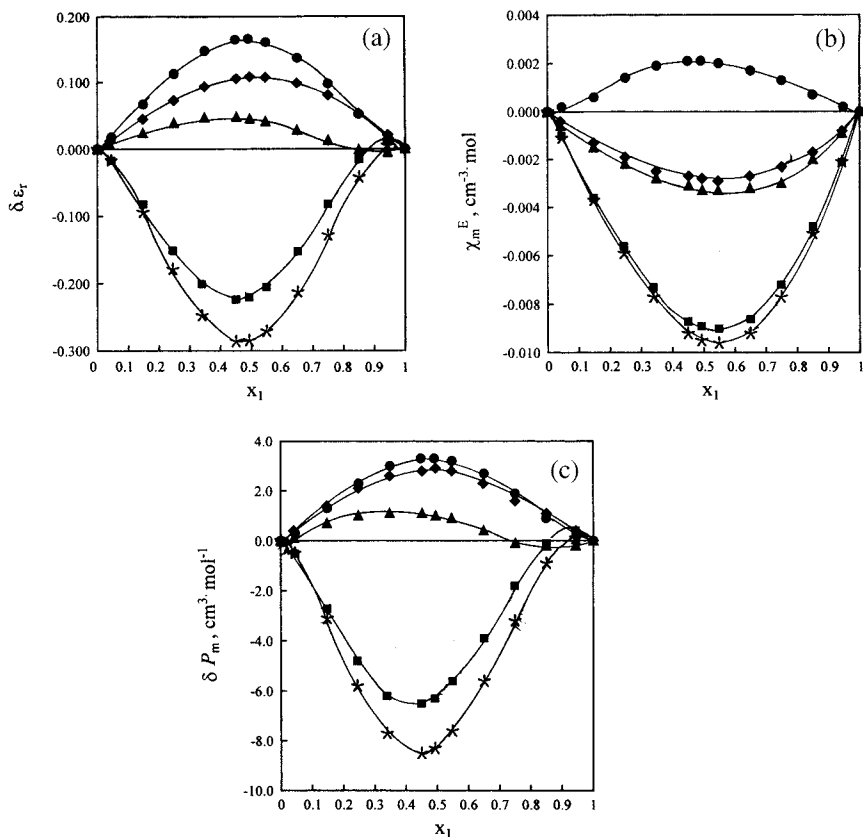


Fig. 3. (a) Deviation in relative permittivities,  $\delta \epsilon_r$ , (b) excess molar electrical susceptibilities,  $\chi_m^E$  and (c) deviation in molar polarizations,  $\delta P_m$  as a function of MMA mole fraction for MMA + di-ethers. (Symbols same as those in Fig. 1.)

for  $g_K$  is characteristic of polar molecules such as MMA. The addition of each of the ethers produced two sets of changes in the  $g_K$  value. For the DEE and DIPE containing mixtures,  $g_K$  values showed an initial increase (up to the region of  $x_1 \approx 0.70$  to  $0.725$ ) and further addition of ethers limits the  $g_K$  values to about 1.28 to 1.30 and 1.28 to 1.29, respectively. However, for the case of DBE addition, the  $g_K$  values showed a continuous decrease and become less than unity at higher DBE compositions. The increase of  $g_K$  values for MMA + DEE and +DIPE mixtures clearly and unambiguously suggests that structure weakening is less in these systems, perhaps due to the dipole-dipole attractive interactions. However, in MMA + DBE systems, the more dominant interaction has always been of

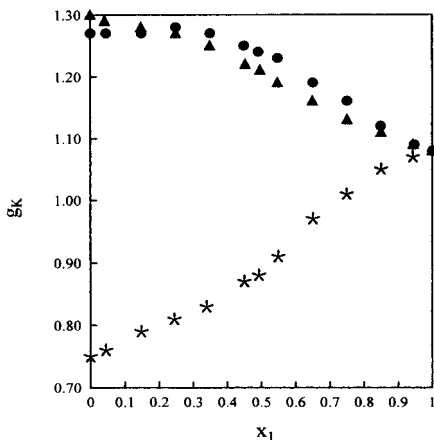


Fig. 4. Variation of Kirkwood correlation factor,  $g_K$  as a function of MMA mole fraction for MMA + aliphatic ethers at  $T = 298.15$  K. (Symbols same as those in Fig. 1.)

the structure weakening type and at higher DBE compositions, while the bulk structures are characterized by  $g_K$  values as small as 0.75 to 0.80, indicating total structure loss in terms of the dipolar arrangement.

## ACKNOWLEDGMENT

The authors thank Prof. Dr. R. M. Patel, Head, Department of Chemistry, Sardar Patel University for providing necessary laboratory facilities.

## REFERENCES

1. N. V. Sastry and P. N. Dave, *Thermochim. Acta* **286**:119 (1996).
2. N. V. Sastry and P. N. Dave, *Int. J. Thermophys.* **17**:1289 (1996).
3. N. V. Sastry and P. N. Dave, *Proc. Ind. Acad. Sci. (Chem. Sci.)* **109**:211 (1997).
4. N. V. Sastry and M. K. Valand, *Int. J. Thermophys.* **18**:1387 (1997).
5. N. V. Sastry and M. K. Valand, *Ber. Bunsenges. Phys. Chem.* **102**:686 (1998).
6. N. V. Sastry and M. K. Valand, *Phys. Chem. Liq.* **38**:61 (2000).
7. N. V. Sastry and S. R. Patel, *Int. J. Thermophys.* **21**:1153 (2000).
8. N. V. Sastry, S. R. Patel, J. George, and D. H. L. Prasad, *Ind. J. Chem. A* **39**:1270 (2000).
9. N. V. Sastry and M. K. Valand, *J. Chem. Thermodyn.* **30**:929 (1998).
10. N. V. Sastry, S. R. Patel, and D. H. L. Prasad, *Thermochim. Acta* **359**:169 (2000).
11. N. V. Sastry, S. R. Patel, and M. C. Patel, *J. Chem. Thermodyn.* **31**:797 (1999).
12. N. V. Sastry, M. C. Patel, and S. R. Patel, *Fluid Phase Equilib.* **155**:261 (1999).

13. G. C. Benson, B. Luo, and B. C.-Y. Lu, *Can. J. Chem.* **66**:531 (1988).
14. L. Wang, G. C. Benson, and B. C.-Y. Lu, *J. Chem. Thermodyn.* **20**:975 (1988).
15. T. Treszczanowicz, *Thermochim. Acta* **160**:253 (1990).
16. L. Wang, G. C. Benson, and B. C.-Y. Lu, *J. Chem. Eng. Data* **35**:242 (1990).
17. A. Jangkamolkuichai, G. C. Alfred, and W. R. Parrish, *J. Chem. Eng. Data* **36**:484 (1991).
18. M. K. Kumaran and G. C. Benson, *J. Chem. Thermodyn.* **18**:27 (1986).
19. L. Wang, G. C. Benson, and B. C.-Y. Lu, *J. Chem. Thermodyn.* **22**:173 (1990).
20. L. Wang, G. C. Benson, and B. C.-Y. Lu, *J. Chem. Thermodyn.* **21**:147 (1989).
21. B. Maronglu, S. Dernini, L. Lepori, E. Matteoli, and H. V. Kehiaian, *J. Chem. Eng. Data* **33**:118 (1988).
22. L. Wang, G. C. Benson, and B. C.-Y. Lu, *J. Chem. Thermodyn.* **21**:61 (1989).
23. P. Berti, L. Lepori, and E. Matteoli, *Fluid Phase Equilib.* **44**:285 (1989).
24. S. T. Blanco, J. M. Embid, and S. Otin, *J. Chem. Thermodyn.* **26**:23 (1994).
25. J. George, N. V. Sastry, and D. H. L. Prasad, *Fluid Phase Equilib.* (in press).
26. N. V. Sastry and M. M. Raj, *J. Soln. Chem.* **25**:1137 (1996).
27. B. Jacobson, *Acta. Chem. Scand.* **6**:1485 (1952).
28. R. Nutsch-Kuhnkie, *Acustica* **15**:383 (1965).
29. W. von Schaaffs, *Acustica* **33**:272 (1975).
30. S. K. Mehta, R. K. Chauhan, and R. K. Dewan, *J. Chem. Soc. Faraday Trans.* **92**:1167 (1996).
31. O. Nomoto, *J. Phys. Soc. Jpn.* **13**:1528 (1958).
32. B. Luo, S. E. M. Hamam, G. C. Benson, and B. C. Y. Lu, *J. Chem. Thermodyn.* **18**:1043 (1986).
33. J. A. Riddick, W. B. Bunger, and T. Sakano, in *Techniques of Chemistry*, Vol. II (John Wiley, New York, 1986).